Effects of Poly(methyl methacrylate)-Based Low-Profile Additives on the Properties of Cured Unsaturated Polyester Resins. I. Miscibility, Curing Behavior, and Glass-Transition Temperatures

Jyh-Ping Dong, Jyh-Gau Huang, Fuh-Huah Lee, Jiunn-Wei Roan, Yan-Jyi Huang

Department of Chemical Engineering, National Taiwan University of Science and Technology, Taipei, Taiwan 106, Republic of China

Received 18 October 2002; accepted 25 August 2003

ABSTRACT: The effects of three series of self-synthesized poly(methyl methacrylate) (PMMA)-based low-profile additives (LPAs), including PMMA, poly(methyl methacrylate-*co*-butyl acrylate), and poly(methyl methacrylate-*co*-butyl acrylate-*co*-maleic anhydride), with different chemical structures and MWs on the miscibility, cured-sample morphology, curing kinetics, and glass-transition temperatures for styrene (ST)/unsaturated polyester (UP) resin/LPA ternary systems were investigated by group contribution methods, scanning electron microscopy, differential scanning calorimetry (DSC), and dynamic mechanical analysis, respectively. Before curing at room temperature, the degree of phase separation for the ST/UP/LPA systems was generally explainable by the calculated polarity difference per unit volume between the UP resin and LPA. During curing at 110°C, the compatibility of the ST/UP/LPA systems, as revealed by cured-sample morphology, was judged from the relative magnitude of the DSC peak reaction rate and the broadness of the peak. On the basis of Takayanagi's mechanical models, the effects of LPA on the final cure conversion and the glass-transition temperature in the major continuous phase of ST-crosslinked polyester for the ST/UP/LPA systems was also examined. © 2004 Wiley Periodicals, Inc. J Appl Polym Sci 91: 3369–3387, 2004

Key words: polyesters; blends; curing of polymers; phase separation; glass transition

INTRODUCTION

The addition of specific thermoplastic polymers as low-profile additives (LPAs) to unsaturated polyester (UP) resins during the formation of sheet-molding and bulk-molding compounds can lead to a reduction or even the elimination of polymerization shrinkage during the cure process.[1,2] Depending on the chemical composition and structure of the UP resins and LPA used, differing degrees of drift in styrene (ST)/UP/LPA compositions, as a result of phase separation during the cure, may occur.[3–7] This can greatly affect the physical and mechanical properties of the cured samples.[7–12]

Suspene et al.[3] studied the miscibility of ST/UP/LPA ternary systems and constructed their cloud-point curves. The cured-sample morphologies were correlated to the ternary system miscibility. Huang and Su[5] also pointed out that the static ternary phase characteristics at 25°C for ST/UP/LPA may be used as a rough guide for accounting for the observed morphology during the reaction at 110°C, where a flake-like or globule microstructure in either the continuous or the dispersed phase can arise. In general, after a phase equilibrium at 25°C for ST/UP/LPA systems, the upper layer (i.e., dispersed phase) was dominated by ST and LPA, whereas the bottom layer (i.e., continuous phase) was dominated by UP and ST. The molar ratio (MR) of ST to polyester C═C bonds in the upper layer was greater than that in the original mixture, whereas the trend was reversed in the bottom layer. A high MR of ST to polyester C═C bonds or a high percentage of LPA may exert profound segregating effects on microgel particles, which can lead to a globule microstructure for the cured sample. In the case of inadequate overall segregating effects on microgel particles, a flake-like microstructure or a coexistence of flake-like and globule microstructures can result.

The objective of this study was to investigate the effects of the chemical structure and molecular weight (MW) of three series of poly(methyl methacrylate) (PMMA)-based LPAs on the miscibility, cured-sample morphology, reaction kinetics, and glass-transition temperatures (T_g's) for ST/UP/LPA ternary systems.

Correspondence to: Y.-J. Huang (yjhuang@ch.ntust.edu.tw).
Contract grant sponsor: National Science Council of the Republic of China; contract grant number: NSC 88-2216-E-011-023.

Journal of Applied Polymer Science, Vol. 91, 3369–3387 (2004)

TABLE I
Raw Materials Used in the Synthesis of PMMA Homopolymer as an LPA

Ingredient	Weight (g)	Moles
Initial solution A of initiator and surfactant		
$K_2S_2O_8$	0.2	0.00074
SDS	5	0.0173
Deionized water	300	—
Initial solution B of monomer and CTA		
MMA	100	1
DM	0.6,[a] 0.36[b]	0.000296,[a] 0.00178[b]

[a] For the synthesis of PMMA1S, a lower MW of LPA.
[b] For the synthesis of PMMA2S, a higher MW of LPA.

The interrelationships between the compatibility, cured-sample morphology, reaction kinetics, and T_g of ST/UP/LPA systems in the major continuous phase of the ST-crosslinked polyester were explored.

EXPERIMENTAL

Synthesis of PMMA-based LPAs

The PMMA-based LPAs with different chemical structures and MWs were isothermally synthesized by emulsion polymerization in either batch or semibatch reactors at 80–90°C for 2–4 h.[13,14] Potassium persulfate ($K_2S_2O_8$) or sodium persulfate ($Na_2S_2O_8$; Acros), nonylphenol polyethoxylate with an average of 40 ethylene oxide units per molecule (NP-40; Union Carbide, Atlanta, GA), and/or sodium dodecyl sulfate (SDS; Acros, Pittsburgh, PA) and dodecyl mercaptan (DM; Acros) were used as the initiator, emulsifiers, and chain-transfer agent (CTA), respectively. The first series of LPAs was made from methyl methacrylate (MMA), the second series of LPAs was made from MMA and *n*-butyl acrylate (BA), and the third series of LPAs was made from MMA, BA, and maleic anhydride (MA). The raw materials used in the synthesis of the six LPAs for this study [PMMA1S, PMMA2S, MMA–BA1S, MMA–BA2S, MMA–BA–MA1S, and MMA–BA–MA2S, where MMA–BA is poly(methyl methacrylate-*co*-butyl acrylate) and MMA–BA–MA is poly(methyl methacrylate-*co*-butyl acrylate-*co*-maleic anhydride)] are summarized in Tables I and II.

A five-necked 2-L glass vessel reactor was used in the synthesis of PMMA-based LPAs. A batch process was used for homopolymer synthesis, and a semibatch process was adopted for copolymer synthesis because of its better control of copolymer composition. For the synthesis of copolymers, an initial solution A (Table II), including deionized water and surfactants, was introduced into the reactor first, stirred for 10 min until the surfactant dissolved in water, where the solution temperature was raised from room temperature to 80°C, and a stirring speed of 400 rpm and a nitrogen sparge rate of 30 mL/min were used. An initial charge B (Table II), consisting of about 10 wt % monomers and CTA, was added into the reactor and was emulsified sufficiently. When the solution temperature was returned back to 80°C, an initiator solution C (Table II) was fed into the reactor. The initial charge was polymerized for about 15 min, and solution D (Table II), which was composed of the remaining deionized water, monomers, surfactant, and CTA, was pumped into the reactor continuously within 3 h at a rate of 2.26 mL/min. After the feeding, the polymerization was continued batchwise for another 30 min. The polymer was precipitated by the addition of methanol into the final latex, coagulated by the addition of 0.5 wt % $Al_2(SO_4)_3$ aqueous solution, filtered for solid product, washed with water to eliminate the surfactant and salt, dried in a vacuum oven at 100°C, and stored for further characterization and use.

For the synthesis of PMMA homopolymer, initial solutions A and B (Table I) were introduced into the reactor and stirred until the surfactant dissolved in water, with the solution temperature maintained at room temperature, a stirring speed of 500 rpm, and a nitrogen sparge rate of 20 mL/min. The temperature was then raised to 80°C, which allowed polymerization to proceed for about 30 min until there was no reflux in the reflux condenser; the temperature was further increased to 90°C and maintained for 2 h for polymerization. The final latex was dried in a vacuum rotary evaporator at 60°C for 8 h. The polymer product in powder form was then dissolved in ST, precipitated by the addition of methanol to the solution, filtered for solid product, washed with water to eliminate the surfactant, dried in a vacuum oven, and stored for further characterization and use.

The properties of the LPAs synthesized in this study are summarized in Table III.

UP resins

The UP resin[6] was made from MA, 1,2-propylene glycol (PG), and phthalic anhydride (PA) with a MR of 0.63 : 1.01 : 0.367. The acid number and hydroxyl number were found to be 28.0 and 28.2, respectively, by end-group titration, which gave a number-average molecular weight (M_n) of 2000 g/mol. On average, the calculated number of C═C bonds in each polyester molecule was 6.79.

Preparation of sample solutions

For the sample solution, 10 wt % LPA was added, and the MR of ST to polyester C═C bonds was fixed at MR = 2 : 1. The reaction was initiated by 1 wt % *tert*-butyl perbenzoate (TBPB; Aldrich).

TABLE II
Raw Materials Used in the Synthesis of MMA–BA and MMA–BA–MA as LPAs

Ingredient	MMA–BA		MMA–BA–MA	
	Weight (g)	Moles	Weight (g)	Moles
Initial solution A of surfactants				
SDS	2.06	0.00715	2.06	0.00715
NP-40	2.07	—	2.07	—
Deionized water	405	—	405	—
Initial solution B of monomers and CTA				
MMA	7.5	0.075	7.5	0.075
BA	17.5	0.136	17.5	0.136
MA	—	—	1.25	0.0128
DM	0.15[a]	0.000743	0.15[c]	0.000743
	0.12[b]	0.000594	0.12[d]	0.000594
Initial solution C of initiator				
$Na_2S_2O_8$	1.67	0.007	1.67	0.007
Deionized water	15	—	15	—
Remaining solution D of surfactant, monomers, and CTA				
Deionized water	80	—	80	—
SDS	7.4	0.0257	7.4	0.0257
MMA	88.5	0.884	88.5	0.884
BA	206.5	1.61	206.5	1.61
MA	—	—	14.75	0.151
DM	1.77[a]	0.00876	1.77[c]	0.00876
	1.416[b]	0.00701	1.416[d]	0.00701
Total feed				
Deionized water	500	—	500	—
SDS	9.46	0.03285	9.46	0.03285
NP-40	2.07	—	2.07	—
MMA	96	0.96	96	0.96
BA	224	1.75	224	1.75
MA	—	—	16	0.1633
DM	1.92[a]	0.00950	1.92[c]	0.00950
	1.536[b]	0.00760	1.536[d]	0.00760
$Na_2S_2O_8$	1.67	0.00702	1.67	0.00702

[a] MMA–BA1S, a lower MW of LPA.
[b] MMA–BA2S, a higher MW of LPA.
[c] MMA–BA–MA1S, a lower MW of LPA.
[d] MMA–BA–MA2S, a higher MW of LPA.

Phase characteristics

To study the compatibility of the ST/UP/LPA systems before the reaction, 20 g of each of the sample solutions was prepared in a 100-mL separatory glass cylinder, which was placed in a constant-temperature water bath at 25 and 110°C. The phase-separation time (t_p) and relative weights of the upper (w_u) and bottom

TABLE III
PMMA-Based LPAs Used in This Study

LPA code	Monomer	Molar composition[a]	M_n[b]	M_w[b]	PD[b]	T_g (°C)[c]
PMMA1S[d]	MMA	—	22,000	71,000	3.2	106
PMMA2S[d]	MMA	—	41,000	119,000	2.9	106
MMA–BA1S	MMA, BA	0.358 : 0.642	20,000	105,000	5.1	−22.7
MMA–BA2S	MMA, BA	0.405 : 0.595	30,000	152,000	5.0	−17.5
MMA–BA–MA1S	MMA, BA, MA	0.340 : 0.611 : 0.049	41,000	79,000	1.9	−23.9
MMA–BA–MA2S	MMA, BA, MA	0.338 : 0.615 : 0.047	49,000	92,000	1.9	−23.9

M_w = weight-average molecular weight.
[a] By ^{1}H-NMR.
[b] By GPC (g/mol).
[c] By DSC.
[d] 1 and 2 denote the lower and the higher molecular weights, respectively.

layers (w_l) were recorded. For the experiment at 110°C, 0.25 wt % of benzoquinone was added as an inhibitor to prevent crosslinking reactions during the experiment.

Cure kinetics

For the cure kinetic study, 6–10 mg of the sample solution was placed in a hermetic aluminum sample pan. The isothermal reaction rate profile at 110°C was measured by a DuPont 9000 differential scanning calorimeter (New Castle, DE), and the final conversion of total C═C bonds at 110°C was calculated.[15]

Scanning electron microscopy (SEM)

The sample solutions were degassed in a vacuum oven at 50°C for 5 min and were then slowly poured into stainless steel rectangular molds with inner trough dimensions of 17 × 1.7 × 0.42 cm and sealed with gaskets. The sample solutions were cured at 110°C in a thermostated silicon oil bath for 1 h and were then postcured at 150°C for another 1 h.

In the morphological study, the cured sample in the mold was removed and broken into several pieces. After the usual sample pretreatment,[5] a Hitachi S-550 scanning electron microscope (Tokyo, Japan) with an accelerating voltage of 20 kV was used to observe the fractured surface of each sample at magnifications of 1000–5000×.

Dynamic mechanical analysis (DMA)

Dynamic mechanical measurements were carried out between −150 and 250°C at 5°C/min and at a fixed frequency of 1 Hz with a DuPont 983 dynamic mechanical analyzer, with rectangular specimens measuring 5 × 1 x 0.2 cm^3 and the same cure temperature history as that of the SEM samples mentioned previously.

RESULTS AND DISCUSSION

Synthesis of PMMA-based LPAs

For MMA–BA copolymer, the introduction of BA can alter the T_g and the molecular polarity in comparison with PMMA. This, in turn, can change the miscibility of the ST/UP/LPA ternary system. For MMA–BA–MA copolymer, the introduction of MA can facilitate the reaction of carboxylic acid group in MA with the thickening agent, such as MgO, during the thickening[16] process in the preparation of polyester molding compounds, and hence, the phase separation of LPAs from the molding compound can be prevented before the cure reaction.

Characterization of LPA

The MMA–BA and MMA–BA–MA molar compositions of LPAs, as shown in Table III, were identified by ^{1}H-NMR, where the peak intensities of —OCH_3 for MMA (δ = 3.5), —OCH_2— for BA (δ = 4.0 ppm), and >CH— for MA (δ = 3.7 ppm) were selected for the calculations.

The M_n, as measured by gel permeation chromatograph (GPC), for the six PMMA-based LPAs fell in the range 20,000–49,000 g/mol, and the polydispersity (PD) generally ranged from 1.9 to 3.2, except for the MMA–BA LPA, which had a PD of about 5.0 (Table III).

The differential scanning calorimetry (DSC) results, as shown in Table III, showed that as the PMMA homopolymer was modified by about 60 mol % BA, the T_g was reduced from 106 to about −20°C.

Interrelationship between the polarity difference of UP and LPA and the compatibility of the ST/UP/LPA systems

The molecular polarities of the UP resin and LPAs were evaluated in terms of the calculated dipole moment per unit volume (μ')[6] with Debye's equation[17] and group contribution methods.[17,18] In general, the higher the polarity difference per unit volume was between the UP and LPA, ($\mu'_{UP} - \mu'_{LPA}$), the lower the compatibility for the ST/UP/LPA system at 25°C before the reaction was. The calculated data in Table IV revealed that the sample solution containing PMMA was theoretically the most compatible, followed by the MMA–BA–MA system and the MMA–BA system. Although this is in agreement with the data in Table IV for the PMMA and MMA–BA systems at 25°C, where the degree of phase separation, as observed from the relative w_u for the former system was lower, the degree of phase separation for the MMA–BA–MA system was the lowest (still one phase after 1440 min), which was not in accord with the theoretical prediction based on the polarity difference between the UP and LPA alone. This was ascribed to the polar interaction between the carboxylic acid group in MA for the MMA–BA–MA LPA and the ester linkage (—COO—) in the UP resin, which led to the best compatibility among the ST/UP/LPA ternary systems.

The relative fractions of both phases, shown in Table IV, depended on the equilibrium compositions (the fractionation of ST and of both polymers between both phases) and the time to attain a condition close to equilibrium. Because the fractions reported in Table IV were measured 1440 min after t_p and remained constant for prolonged periods of time, w_u and w_l should have been close to the equilibrium values.

Factors affecting the rate of decantation of both liquid phases at 25°C were the viscosities of both

TABLE IV
Calculated Molar Volumes (V's) and Dipole Moments (μ) for the UP Resin and LPAs and Phase Characteristics of ST/UP/LPA Uncured Systems at 25 and 110°C

	μ (Debye/mol$^{1/2}$)	V (cm^3/mol)	μ'[a]	$\mu'_{UP} - \mu'_{LPA}$	t_p (min) at 25°C	W_u at 25°C[b]	W_l at 25°C	t_p (min) at 110°C
UP resin								
MA–PG–PA	3.13	1,389	0.0840	—				
LPAs								
PMMA1S	9.69	18,110	0.0720	0.0120	95	20.2	79.8	>180
PMMA2S	13.22	33,710	0.0720	0.0120	40	28.4	71.6	>180
MMA–BA1S	8.50	17,480	0.0643	0.0197	480	33.6	66.4	>180
MMA–BA2S	10.47	26,110	0.0648	0.0192	1320	40.0	60.0	>180
MMA–BA–MA1S	12.41	34,840	0.0665	0.0175	>1440	—[c]	—	>180
MMA–BA–MA2S	13.55	41,690	0.0664	0.0176	>1440	—[c]	—	>180

[a] $\mu^2/v^{1/2}$ (Debye/cm$^{3/2}$).
[b] Measured at 1440 min after t_p, where it then remained constant for long periods of time.
[c] Single phase.

phases and the difference in densities, where lower viscosities and a larger difference in densities may have enhanced the rate of phase separation of the ST/UP/LPA systems. Table IV shows that the rate of phase separation at 25°C was much faster for the PMMA system than for the other two systems. Our explanation is that PMMA was in the glassy state at room temperature (T_g = 106°C), which was in contrast with MMA–BA and MMA–BA–MA in the rubbery states (T_g = −17 to −24°C, as listed in Table III), and the viscosity of the ST/UP/LPA system containing PMMA was much lower than those of the MMA–BA and MMA–BA–MA systems, which led to a much faster rate of phase separation for the former system.

Table IV also shows that for a fixed type of LPA, the addition of a higher MW LPA may have enhanced the degree of phase separation, as revealed by the higher relative weight percentage for the upper layer solution after a phase equilibrium, but may have either increased (for the less viscous PMMA system) or decreased (for the more viscous MMA–BA system) the phase-separation rate. Because increasing the MW of LPA may have enhanced both the viscosities, as mentioned earlier, and the difference in densities of both phases, because of the higher degree of phase separation, we inferred that the effect of viscosity was predominant over that of the density difference on the phase-separation rate for the more viscous MMA–BA–MA system, which led to a longer t_p for the higher MW LPA. In contrast, the trend was reversed for the less viscous PMMA system.

As the mixing temperature was increased from 25 to 110°C, no phase separation was observed for all six of the ST/UP/LPA ternary systems within 180 min (Table IV), after which they started to polymerize despite no addition of the TBPB initiator in the system. As shown later, for the ST/UP/LPA system with the TBPB initiator added, the reaction at 110°C isothermally ended in 60 min. Therefore, all six of the systems in this study exhibited a single homogeneous phase after a phase equilibrium before the reaction at 110°C.

The higher the mixing temperature was, the more compatibile was the ST/UP/LPA ternary system containing PMMA as an LPA over the temperature range 25–110°C, as evidenced by a longer t_p (40–95 min vs. at least 180 min). Hence, the ST/UP/LPA ternary systems containing relatively nonpolar PMMA-based LPAs in this study, such as PMMA1S and PMMA2S, possessed an upper critical solution temperature instead of a lower critical solution temperature.

Relationship between the compatibility of ST/UP/LPA systems and cured-sample morphology

During the cure at 110°C, the sample solution containing PMMA was the most compatible, followed by the MMA–BA–MA system and the MMA–BA system, which was in agreement with the prediction based on the calculated polarity difference of UP and LPA mentioned previously. This was evidenced by the SEM micrographs [Fig. 1(a–d)], which showed a cocontinuous globule morphology containing a crosslinked polyester phase (or microgel particle phase) and an LPA-rich phase for the PMMA1 system and a two-phase microstructure consisting of a flake-like continuous phase and a globule LPA-dispersed phase for both the MMA–BA–MA and MMA–BA systems. The MMA–BA–MA system was more compatible than the MMA–BA system during the cure because the number of LPA-dispersed phases was fewer for the former system [compare Fig. 1(b–c) and 1(d)].

With a fixed type of LPA, the addition of a higher MW LPA caused a lower compatibility of the ST/UP/LPA system during the cure. For the sample solution containing PMMA, the addition of a higher MW LPA caused the change of cured-sample morphology from a cocontinuous globule morphology to an underdeveloped two-phase microstructure (not shown). In con-

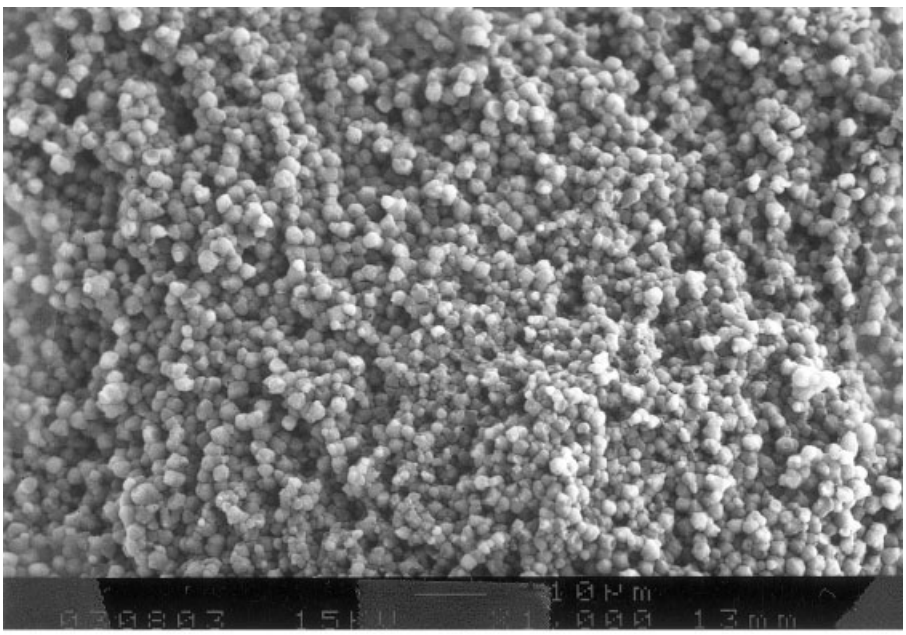

(a)

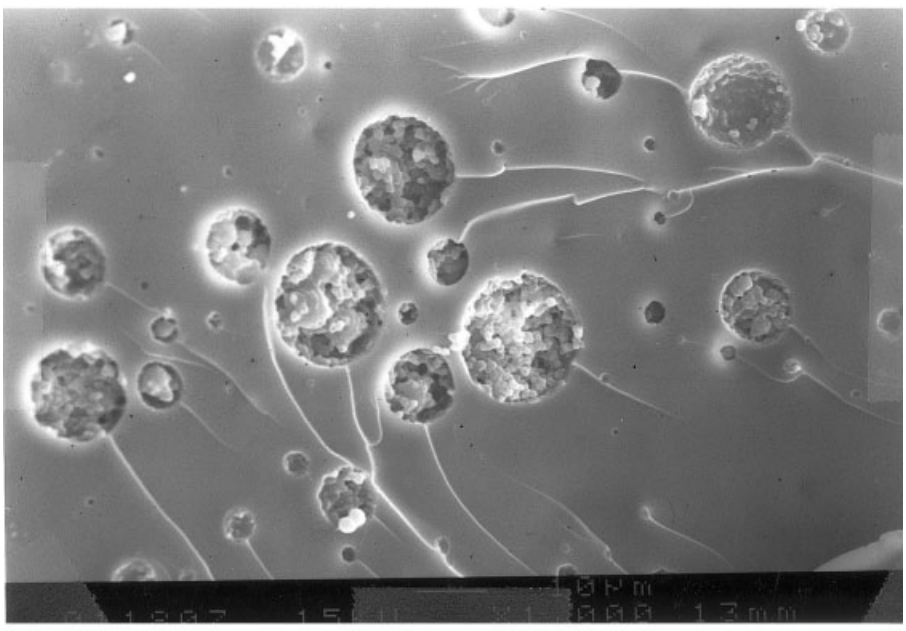

(b)

Figure 1 SEM micrographs (obtained at 1000×) of the fractured surfaces for cured UP resins containing 10% PMMA-based LPAs: (a) PMMA1S, (b) MMA–BA1S, (c) MMA–BA2S, and (d) MMA–BA–MA1S.

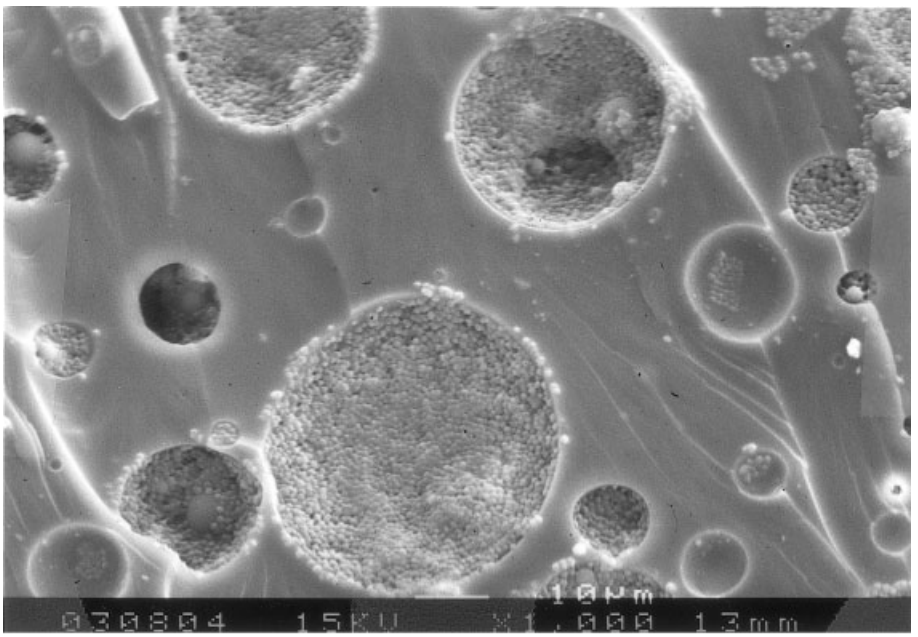

(c)

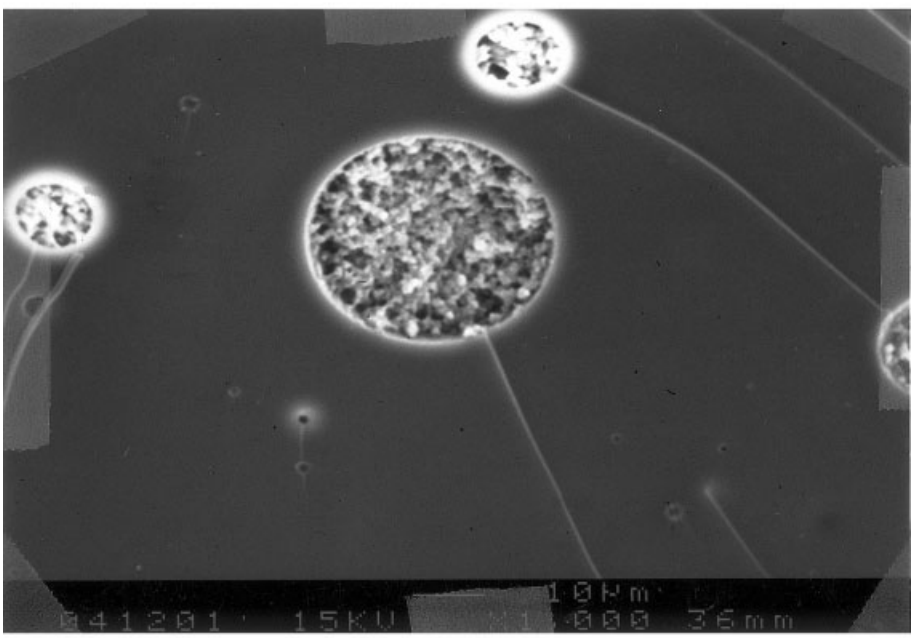

(d)

Figure 1 (*Continued from the previous page*)

trast, for the sample solutions containing MMA–BA and MMA–BA–MA, the addition of a higher MW LPA resulted in either a larger average domain size in the dispersed phase for the former system [compare Figs. 1(b) and 1(c)] or a greater number of dispersed phases for the latter system (not shown) during the cure.

Strictly speaking, to assess the compatibility of different additives, it was necessary to determine the cloud-point temperatures[3,19] for the four additives that were not miscible at 25°C and the cloud-point conversions[3–5,20] at 110°C for the six additives. It was not safe to estimate compatibility by the SEM micrographs at full conversion.

Relationship between morphologies and mechanical properties: the Takayanagi models

For the cured LPA-containing UP resin systems with morphologies as shown in Figure 1(a–d), their mechanical behavior could be approximately represented by the Takayanagi models,[11,21–23] where arrays of weak LPA (R) and stiff ST-crosslinked polyester (P) phases are indicated (see Fig. 2). The subscripts 1, 2, and 3 for the P phases are used because of the distinction of ST and UP compositions as a result of phase separation during cure, and the quantities λ, ϕ, ξ, and ν or their indicated multiplications indicate the volume fractions of each phase.

For the systems shown in Figure 1(a), the microgel particles (phase P_1) were surrounded by a layer of LPA (phase R). Between the LPA-covered microgel particles, there were some lightly ST-crosslinked polyester chains and polystyrene chains (taken both together as phase P_2), with different compositions of ST and UP from those in phase P_1, dispersed in the LPA phase (phase R). Hence, the characteristic globule microstructure could represented by the parallel–parallel–series (P–P–S) model, as shown in Figure 2(a), which is a parallel combination of the three elements, that is, P_1, R, and P_2–R in series. In contrast, for the system shown in Figure 1(b–d), the microstructure consisted of a stiff continuous phase of the ST-crosslinked polyester (phase P_1) and a weak globule LPA-dispersed phase, whose globule morphology could also be represented by a P–P–S model. Hence, the upper bound of mechanical behavior for the overall morphology could be represented by a parallel–parallel–parallel–series [P–(P–P–S)] model, as shown in Figure 2(b), which is simply a parallel combination of the continuous phase P_1 and the dispersed phase denoted by a P–P–S model.

The mechanical properties of cured samples could change not only with the morphology but also with the crosslinking density of the ST-crosslinked polyester in the P_1, P_2, and P_3 phases, with the major continuous phase P_1 being the dominant one. The latter information was not easily obtained but could be inferred from the static phase characteristics of the ST/UP/LPA systems at 25°C before curing.[5]

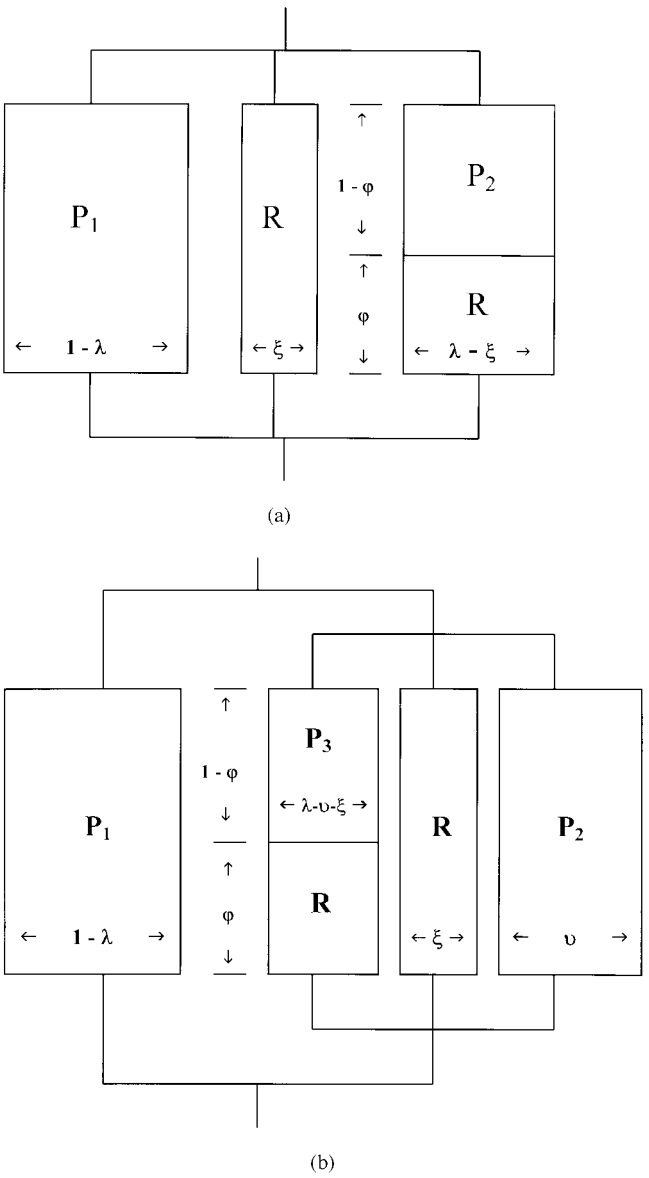

Figure 2 Takayanagi models for the mechanical behavior of cured LPA-containing UP resin systems: (a) P–P–S and (b) P–(P–P–S) models. The area of each diagram is proportional to a volume fraction of the phase.

Effects of drift in ST/polyester compositions on the reaction rate during curing

Figure 3 shows the DSC reaction rate profiles at 110°C for ST/UP/LPA systems. As pointed out by Huang and Lee,[24] the ST/UP reaction may experience an induction time or inhibition time (~10 min as shown in Fig. 3) because of the existence of inhibitor in the system. The initial increase in the reaction rate after the inhibition period was mainly due to the increase in active chains (or the free-radical concentration), a

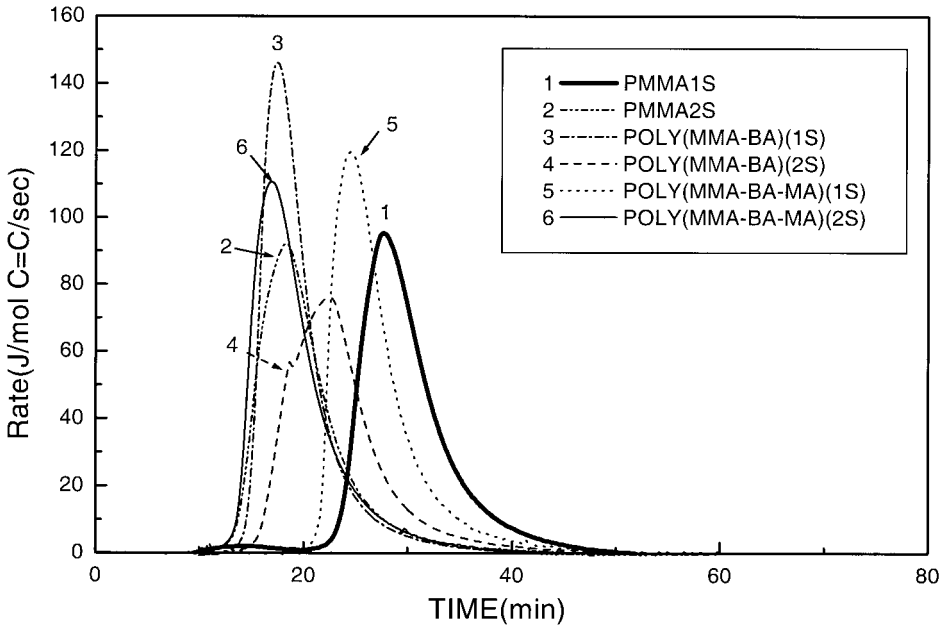

Figure 3 Effects of LPA type on the DSC reaction rate profile at 110°C for ST/UP/LPA systems.

well-known effect in these polymerizations. The reaction could then reach a maximum reaction rate because of the gel effect caused by the diffusion-controlled termination of polymeric radical chains. The reaction rate decayed rapidly at the later state of cure because of the glass-transition effect caused by the diffusion-controlled propagation of ST and UP C═C bonds.

For the most incompatible MMA–BA2S system during the cure, as evidenced by the SEM micrograph in Figure 1(c), the reaction rate profile exhibited a remarkable shoulder first, which occurred at a time of 18.6 min with a conversion of 0.093, followed by a major peak, which occurred at a time of 22.7 min with a conversion of 0.38. As a result of phase separation during the cure for the ST/UP/LPA system with a MR of ST to polyester C═C bonds of 2 : 1 and 10 wt % LPA, the noticeable shoulder of the DSC rate profile before the major peak was mainly due to the gel effect in the flake-like continuous phase, in which the MR was smaller than 2 : 1, whereas the peak of the rate profile was mainly due the gel effect in the globule LPA-dispersed phase, in which the MR was greater than 2 : 1. This was in contrast to a single major peak in the rate profile for the other five systems with moderate phase-separation phenomena during the cure, where the onset of gel effects in the major continuous phase and the LPA-dispersed phase were so close that the peak reaction rates for the two phases were overlapped with each other.

Horie et al.[25] pointed out that for the copolymerization of diethyl fumarate (monomer 2) and ST (monomer 1), the reactivity ratios were $r_1 = 0.30–0.40$ and $r_2 = 0.07–0.09$ at 60–130°C. Therefore, the reaction rate for the copolymerization of ST with polyester C═C bonds was greater than that of the self-bonding of ST, as also reported by Huang et al.[26] Indeed, for ST/UP/PMMA systems, it was reported[20] that during the cure, the flake-like continuous phase with MR $< 2 : 1$ gelled first, whereas the LPA-dispersed phase with MR $> 2 : 1$ lagged behind. Therefore, for the six ST/UP/LPA systems, the onset of the gel effect or the autoacceleration effect should have occurred earlier for the major continuous phase, in which ST concentration was lower, than for the LPA-dispersed phase, in which ST concentration was higher.

As a result of phase separation during the cure, the distribution of initiator and inhibitor between the major continuous phase and the LPA-dispersed phase (or LPA cocontinuous phase) was disregarded here for simplicity of the analysis. Also, the effects of the type and MW of LPA on the molecular or segment mobilities (microviscosity) and the resulting rate of termination in the different phases on peak reaction rate were not taken into account here. Although this may have affected the onset of the gel effect and the peak reaction rate for different phases during the cure somewhat, the MR of ST to polyester C═C bonds (MR) therein, which affected the propagation rate constants for the free-radical crosslinking copolymerization of ST and polyester C═C bonds, should have been the dominating factor for them. This is because for the highly crosslinking ST/UP reaction system, the onset of diffusion-controlled termination occurred at the early stage of the reaction,[24] which was verified by electron spin resonance studies.[27] Unlike a linear polymerization system, such as ST polymerization, where the peak rate of the DSC profile may be greatly

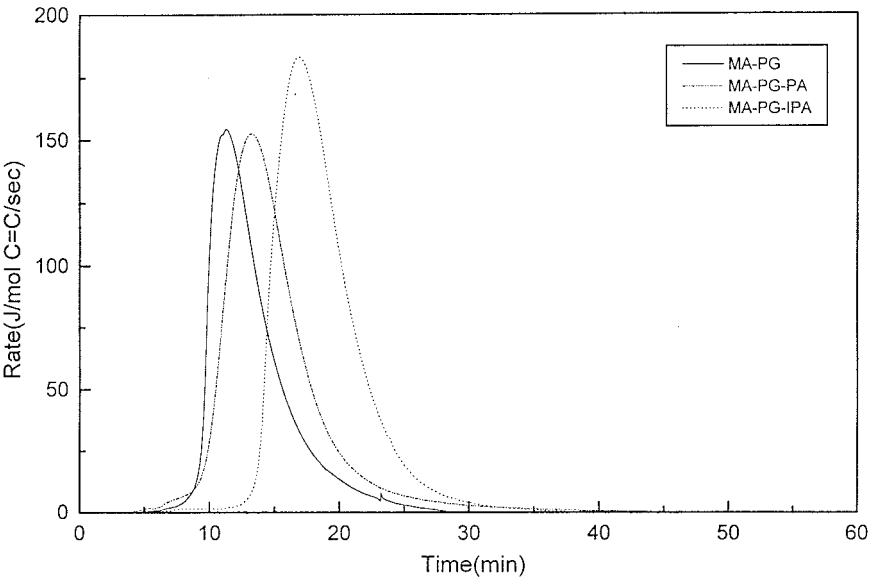

Figure 4 Effects of UP type on the DSC reaction rate profile at 110°C for ST/UP systems (MR = 2 : 1). Three UP resins were used,[6] including MA–PG, MA–PG–PA, and MA–PG–isophthalic acid (IPA). Final α values of 81.3, 91.8, and 84.8%, respectively, were obtained.[29]

influenced by the rate of termination,[24] the difference in the effect of the termination reaction on the peak rate among the ST/UP/LPA systems was much less than that of the effect of the propagation reaction.

Figure 3 also reveals that for a fixed type of LPA, the addition of a higher MW LPA may have enhanced the degree of phase separation during the cure, as inferred from the lower peak reaction rate and the wider rate profile around the peak. This was because the less compatible ST/UP/LPA system caused by the addition of a higher MW LPA during the cure led to a greater deviation from a MR of 2 : 1 in either the major continuous phase (i.e., phase P_1 in Fig. 2), where the MR was smaller than 2 : 1, or the LPA-dispersed phase (i.e., phases P_2 and P_3, and R as a whole in Fig. 2), where the MR was larger than 2 : 1, and hence, the onset of the gel effect for the two phases could not coincide, which led to a broadening of the peak and a lowering of the peak reaction rate.

For the ST/UP reaction, the peak reaction rate reached a maximum at MR = 2 : 1, below or above which the peak reaction rate could have decreased.[28] Indeed, as result of phase separation during cure, the peak reaction rate for the ST/UP/LPA systems shown in Figure 3, which is a summation of reaction rates in the major continuous phase and the LPA-dispersed phase (or LPA cocontinuous phase), was smaller than that for the neat MA–PG–PA UP resin[29] (Fig. 4) without phase separation during the cure (<150 vs. >150 J/mol C═C/s).

Cloud point during the cure

As shown in Figure 3, there was a shift in the time scale produced by a change in the MW of the same additive. The location of the cloud-point time (t_{cp}; i.e., the onset of noticeable phase separation) corresponded to the very low cure conversion ($\alpha < 1\%$),[5] which was solely inferred from the detailed morphological changes during the entire cure reaction for the typical ST/UP/PMMA system. (Experiments were not carried out for the six systems.) As a first approximation, the time to reach a α of 1% (t_{cp}), on the basis of the DSC conversion profile in Figure 5, was taken as the time approximating the t_{cp}. Figure 5 reveals that for the PMMA and MMA–BA–MA systems, t_{cp} was smaller when a higher MW LPA was added (18.6 vs. 12.1 min for the PMMA system and 22.0 vs. 12.1 min for the MMA–BA–MA system), whereas the trend was reversed for the MMA–BA systems (13.2 vs. 16.4 min).

The shift for times approximating to t_{cp} were caused by the distribution of initiator and inhibitor between the major continuous phase and the LPA-dispersed phase (or LPA cocontinuous phase). In general, the more pronounced the phase separation for the ST/UP/LPA system was, the lower the concentration of inhibitor in the major continuous phase was, which led to a smaller t_{cp}. This was because the cure reaction occurred earlier in the major continuous phase than that in the LPA-dispersed phase because of the shorter inhibition time for the former phase. Besides, the cure reaction rate was also faster in the major continuous phase because of a lower ratio of ST to polyester C═C bonds (MR) therein, which caused an earlier onset of noticeable phase separation. This was the reason why at a fixed LPA, t_{cp} was reduced by an increase in the MW of LPA, such as with PMMA and MMA–BA–MA, for the ST/UP/LPA systems during the cure, where the ternary system with a higher MW LPA added

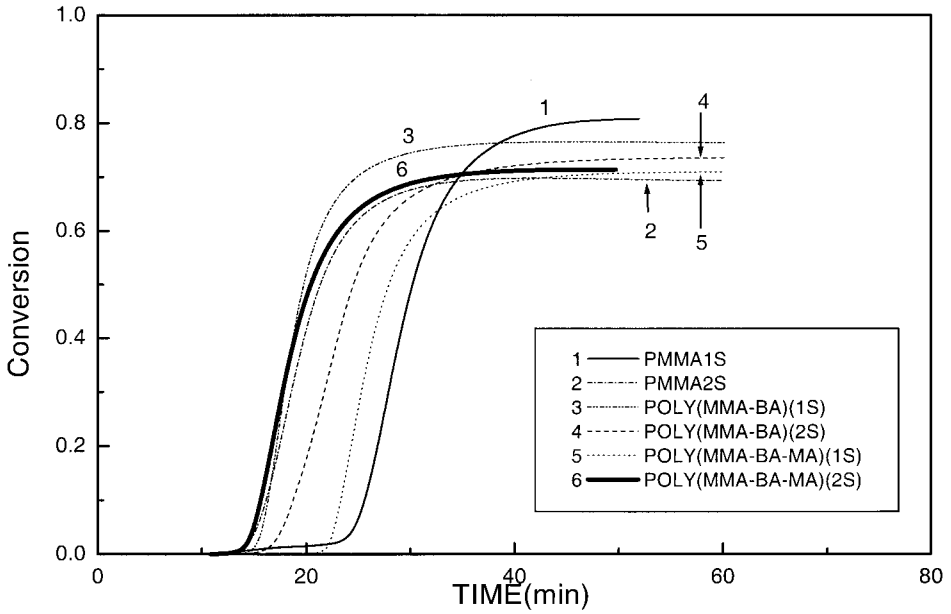

Figure 5 Effects of LPA types on the DSC conversion profile at 110°C for ST/UP/LPA systems.

became more incompatible. However, the ST/UP/LPA system containing MMA–BA showed an opposite trend, which was ascribed to the viscosity increase caused by the increasing MW of the LPA and the concomitant slower phase-separation rate for the ST/UP/LPA system during the cure, which led to a longer inhibition time in the major continuous phase.

The trend of the phase-separation rate for the ST/UP/LPA system during the cure was in agreement with that for the uncured ST/UP/LPA systems at 25°C, where increasing the MW of LPA also led to an increase in the phase-separation rate (t_p) for the MMA–BA system rather than a decrease in t_p for the PMMA system (Table IV). Therefore, the static ternary phase characteristics at 25°C for the uncured ST/UP/LPA system could be used as a rough guide for accounting for the phase-separation phenomenon during the reaction at 110°C.

Effects of the phase-separation behavior and T_g of LPA on α

Figure 5 shows the DSC conversion profiles of total C═C bonds at 110°C for the ST/UP/LPA system. The final conversion was incomplete because of both the glass-transition effect, where the vitrification of the reacting phases led to a halt of the propagation reaction, and the shielding wall effect, to be explained later.

The T_g's for the ST/UP/LPA system corresponding to full cure (i.e., 110°C for 1 h and 150°C for another 1 h, after which the reaction had ceased), to be discussed in the next section, are listed in Table V. Here, we define an index of the glass-transition effect at different phases during the cure at 110°C, ΔT_{Pi}, which was the difference between the glass-transition temperature of phase P_i corresponding to full cure (T_{gi})

TABLE V
T_g Values of Fully Cured ST/UP/LPA Systems on the Basis of Tan δ measured by DMA

LPA	MR	Model	$T_{g1\alpha}$	$T_{g1\beta}$	T_{g2}	T_{g3}	T_{gR}
Neat UP resin							
	1 : 1		148.0	88.5			
	2 : 1		162.4	115.6			
	3 : 1		158.1	97.7			
	6 : 1		143.7	—			
LPA							
PMMA1S	2 : 1	P–P–S	165.1	—	124.1		—
PMMA2S	2 : 1	P–(P–P–S)	159.5	—	127.2	—	—
MMA–BA1S	2 : 1	P–(P–P–S)	164.7	—	122.6	—	—
MMA–BA2S	2 : 1	P–(P–P–S)	161.4	—	125.2	18.9	—
MMA–BA–MA1S	2 : 1	P–(P–P–S)	159.5	—	123.4	—	—
MMA–BA–MA2S	2 : 1	P–(P–P–S)	160.6	—	111.5	—	—

and the isothermal cure temperature at 110°C (T_{cure}). As revealed in Table V, for the PMMA1S and PMMA2S systems with a T_g of LPA at 106°C, all of the phases could vitrify during the cure at 110°C, where $\Delta T_{Pi} > 0$ (i.e., $T_{gi} > T_{cure}$), whereas for the other four systems with a T_g of LPA ranging from −17 to −24°C, only the P_3 phase could not vitrify during the cure at 110°C, where ΔT_{P1} and $\Delta T_{P2} > 0$ but $\Delta T_{P3} < 0$. (For the MMA–BA1S and MMA–BA–MA systems, the T_g for the P_3 phase at the end of cure appeared to occur at −10 to 25°C, as shown by the DMA results in the next section.) A limited isothermal α at 110°C occurred for the P_1 and P_2 phases and, hence, for the whole sample of the ST/UP/LPA system. (The P_3 phase occupied only a small portion of the sample, and even the 100% monomer conversion therein could not compensate for the limited conversion in the other phases.)

For the inhomogeneous ST-crosslinked polyester network, even after the material was scanned to a temperature at which all reaction had ceased, as mentioned earlier, residual C═C bonds remained,[29] especially for the polyester C═C bonds. This was ascribed to the shielding wall effect,[15] which prevented the ST monomers from further diffusing into the interior of microgels and greatly curtailed the final conversion of C═C units because of the incomplete intramicrogel crosslinking reactions. This was in contrast to a linear polymerization system, such as ST polymerization, where a 100% monomer conversion can be achieved as long as the polymerization temperature exceeds the T_g of its polymer.[24]

For ST/UP/LPA systems, the final conversion ranged from 69.9 to 80.6% (Fig. 5), which was lower than that of the neat MA–PG–PA UP resin (α = 91.8% as measured by DSC and α = 87.3% as measured by Fourier transform infrared spectroscopy).[29] The decreasing order of final conversion for the ST/UP/LPA systems was generally PMMA1S > MMA–BA > MMA–BA–MA > PMMA2S (Fig. 5). This seemed to reveal that the most compatible PMMA1S system during the cure with a cocontinuous globule morphology may have had the highest final conversion after the cure. In contrast, for the systems with two-phase cured-sample morphologies, such as PMMA2S, MMA–BA, and MMA–BA–MA, Figure 5 appears to indicate that the less compatible the ST/UP/LPA system was during the cure, the higher the final conversion after the cure was.

In fact, the total α was a summation of the α's in phases P_1, P_2, and P_3, as shown in Figure 2(b). It depended on the molar ratio in each phase as a result of phase separation during the cure (MR_{Pi}), which was associated with the shielding wall effect, and ΔT_{Pi}, which was associated with the glass-transition effect.

In general, for the ST/UP/LPA systems, if the MR deviated more from (less than) 2 : 1 in the major continuous phase (i.e., phase P_1 in Fig. 2) during curing, a more compact microgel structure in that phase resulted, which led to a lower α therein. [Our previous research[15] showed that the lower the MR of ST to polyester C═C bonds (MR) was, the lower the final conversion was because of the worse swelling effect of ST on the microgel structures or the more pronounced shielding wall effect.] However, a lower MR in the P_1 phase was accompanied by higher MRs in the P_2 and P_3 phases as a result of phase separation during the cure. This may have reduced the T_g in the P_2 and P_3 phases, where MR > 2 : 1. A decrease in ΔT_{Pi} in the P_2 and P_3 phases could thus result in an increase in α therein. Because the final conversion depended on the combination of the fractionation of different species among different phases and the vitrification of one or more of these phases, no prediction could be made with regard to the effect of LPA type on final conversion for the systems studied.

In contrast to the effect of the chemical structure of LPA on α, for a fixed type of LPA, the addition of a higher MW LPA generally resulted in a decrease in the final conversion (Fig. 5). This was because of the lower compatibility of the ST/UP/LPA system and the associated lower α caused by a greater shielding wall effect in the P_1 phase, which dominated the final α.

Crosslinking density effect and plasticization effect on the T_g of the P phase

Figure 6 shows the DMA results for the cured neat UP resins without LPAs at varied MRs of ST to polyester C═C bonds. On the basis of the tan δ curve of DMA, the maximum point at higher temperatures was identified as the glass-transition temperature for the overall ST-crosslinked polyester matrix ($T_{g1\alpha}$), whereas the shoulder at lower temperatures was identified as the β relaxation temperature ($T_{g1\beta}$)[30] for the polyester segments between the crosslinks alone. In our opinion, $T_{g1\beta}$ could also be affected by the motion of chain segment of the ST bridge between the crosslinks.

The T_g values displayed in Table V reveal that as the MR increased, $T_{g1\alpha}$ exhibited an increase, followed by a decrease, and reached a maximum at MR = 2 : 1 ($T_{g1\alpha}$ = 162.4°C), which showed a similar trend to those reported in the literature.[31,32] Similarly, $T_{g1\beta}$ also reached a maximum at MR = 2 : 1 ($T_{g1\beta}$ = 115.6°C) in this study. At MR = 6 : 1, $T_{g1\beta}$ could not be identified [Fig. 6(d)].

On one hand, the higher the MR was, the higher the degree of crosslinking was along the polyester chain, as evidenced by the higher conversion of polyester C═C bonds,[15] which led to a favorable effect on the increase of $T_{g1\alpha}$ and $T_{g1\beta}$. However, the higher the MR was, the longer the ST bridge between the crosslinks (i.e., the crosslink length of ST) was,[28] which resulted in an adverse effect on the increase of $T_{g1\alpha}$ (because of the decrease in overall crosslinking density) and $T_{g1\beta}$

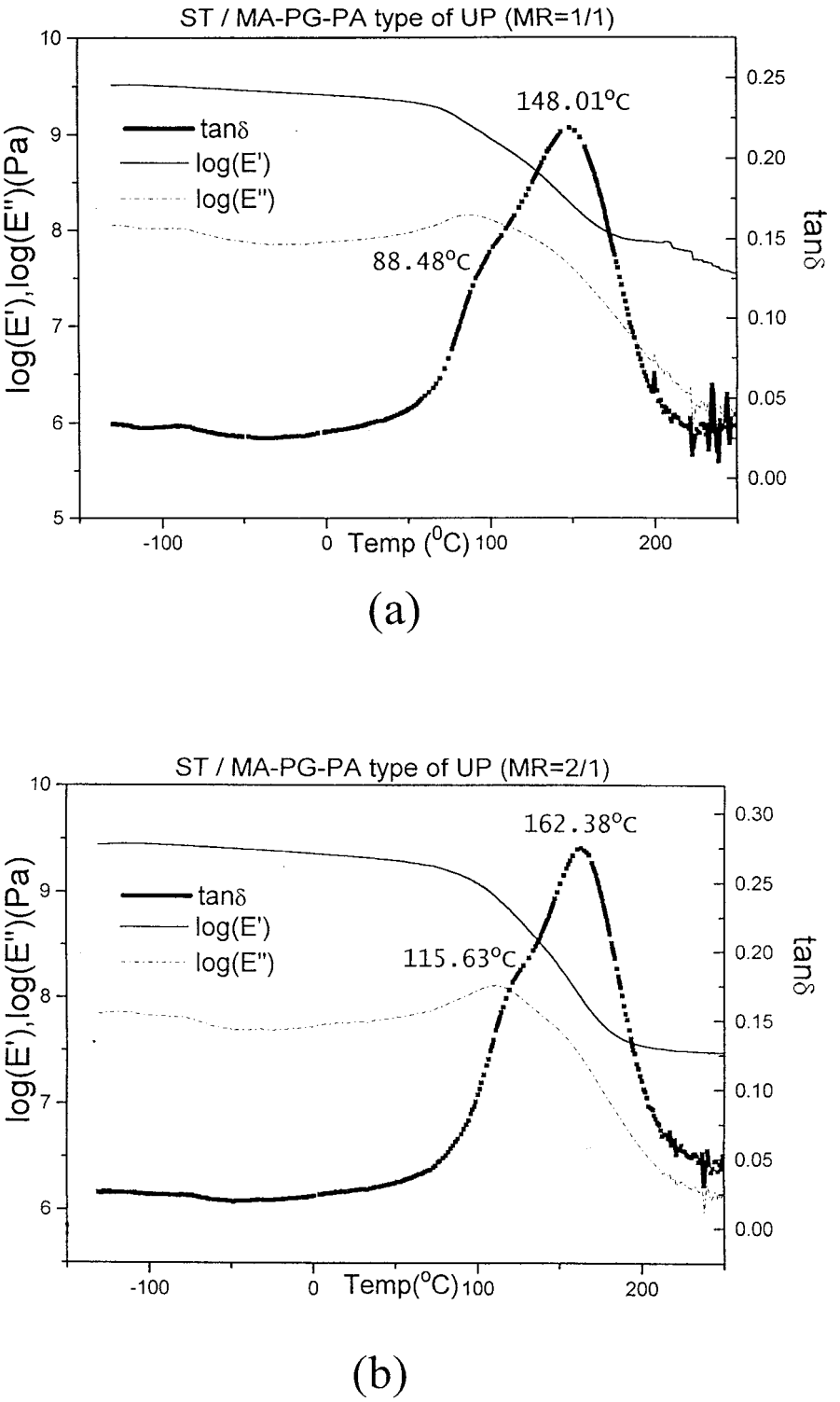

Figure 6 Storage modulus (E'), loss modulus (E''), and tan δ versus temperature for cured neat UP resins at varied MRs of ST to polyester C═C bonds (MR) by DMA: MR = (a) 1 : 1, (b) 2 : 1, (c) 3 : 1, and (d) 6 : 1.

(because of the lower restriction for the ST bridge to the mobility of polyester chain segments between the crosslinks). For the ST-crosslinked polyester matrix, the crosslinking density reached an optimum at an MR of 2 : 1, below or above which, the crosslinking density could be reduced, and hence, maximum $T_{g1\alpha}$ and $T_{g1\beta}$ were observed at MR = 2 : 1.

Figure 7 shows the DMA results for the cured UP resins containing 10 wt % LPA. Although a P–P–S model [Fig. 2(a)] was proposed for the most compat-

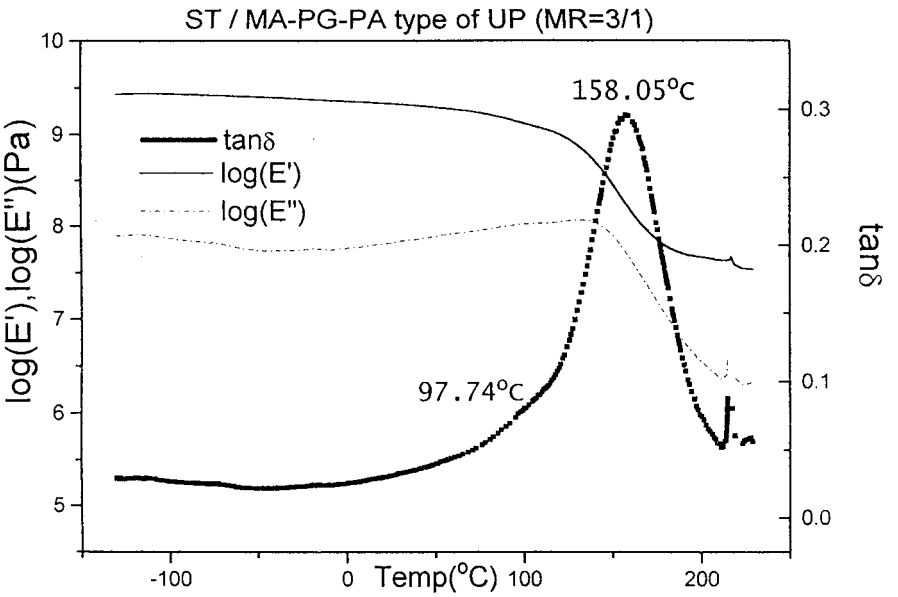

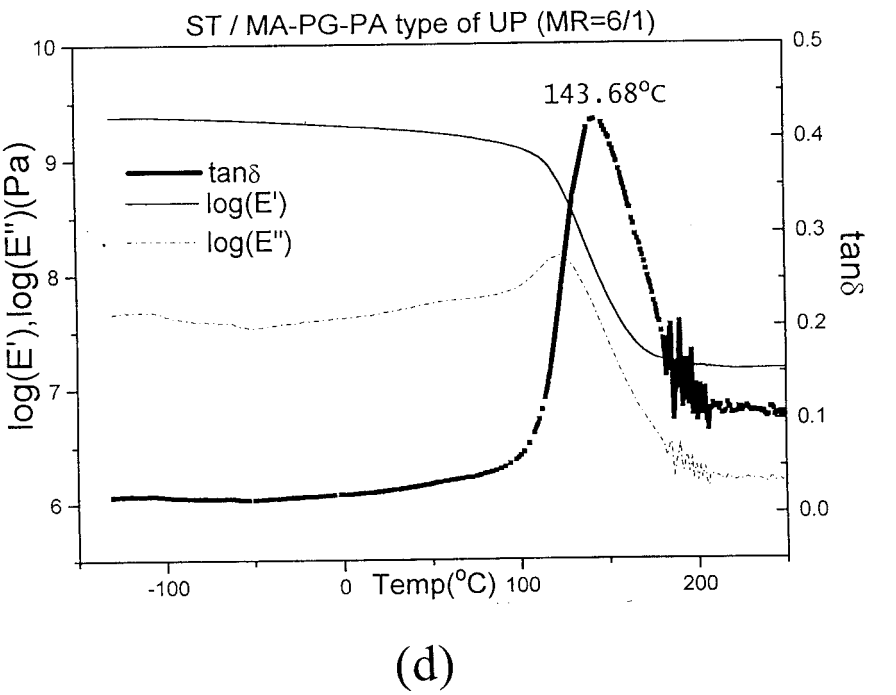

Figure 6 (*Continued from the previous page*)

ible PMMA1S system and a P–(P–P–S) model [Fig. 2(b)] was proposed for the other five systems, for almost all of the systems, only the T_g at the P_1 phase at 159–166°C and the glass-transition temperature at the P_2 phase (T_{g2}) at 111–128°C could clearly be identified. The glass-transition temperature at the P_3 phase (T_{g3}) could also be identified unambiguously at 19°C for the most incompatible MMA–BA2S system, whereas that for the MMA–BA1S and MMA–BA–MA systems with two-phase microstructures similar to that of the MMA–BA2S system, which appeared to be around −10 to 25°C, could not be clearly identified. T_{g3} and

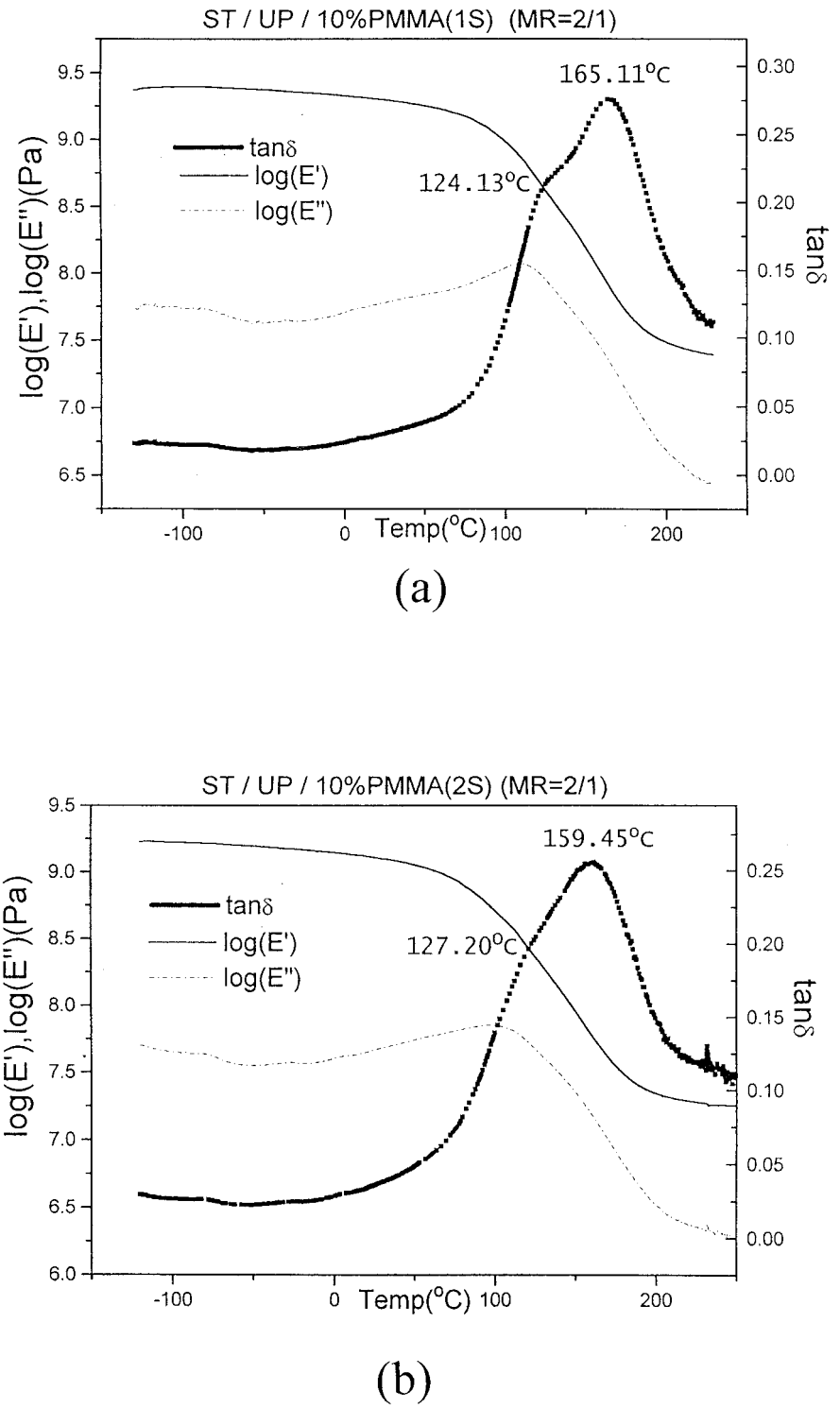

Figure 7 Storage modulus (E'), loss modulus (E''), and tan δ versus temperature for cured ST/UP/LPA systems containing 10% LPA at MR = 2 : 1 by DMA: (a) PMMA1S, (b) PMMA2S, (c) MMA–BA1S, (d) MMA–BA2S, (e) MMA–BA–MA1S, and (f) MMA–BA–MA2S.

the glass-transition temperature of the R phase (T_{gR}) generally remained unidentified.

In Table V for the ST/UP/LPA cured systems, $T_{g1\alpha}$ is the glass-transition temperature for the major continuous phase of the ST-crosslinked polyester (i.e., phase P_1 in Fig. 2), $T_{g1\beta}$ (°C) is the β relaxation temperature for the polyester segments between the crosslinks mainly in the densely ST-crosslinked polyester phase [i.e., phase P_1 in Fig. 2(a) and phases P_1 and P_2 in Fig. 2(b)], T_{g2} is the glass-transition temper-

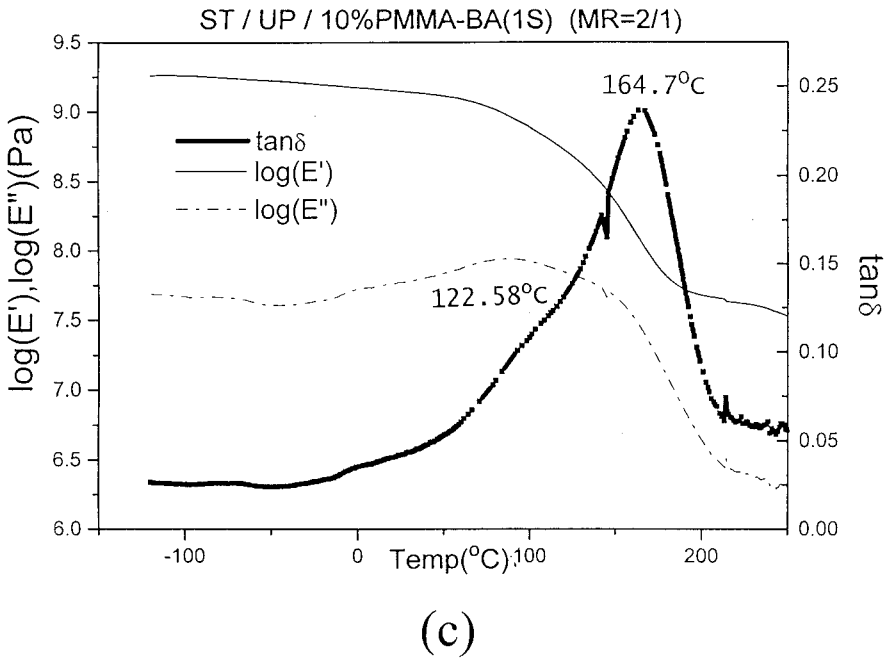

Figure 7 (*Continued from the previous page*)

ature for either the LPA cocontinuous phase [i.e., phase P_2 in Fig. 2(a)] or the major microgel particle phase within the LPA-dispersed phase [i.e., phase P_2 in Fig. 2(b)], T_{g3} is the glass-transition temperature for the LPA cocontinuous phase within the LPA-dispersed phase [i.e., phase P_3 in Fig. 2(b)], and T_{gR} is the glass-transition temperature of the R phase. For the PMMA1S and PMMA2S systems [Fig. 7(a, b)], T_{gR} (106°C as measured by DSC) could be superposed with T_{g2}. Similarly, for the MMA–BA and MMA–

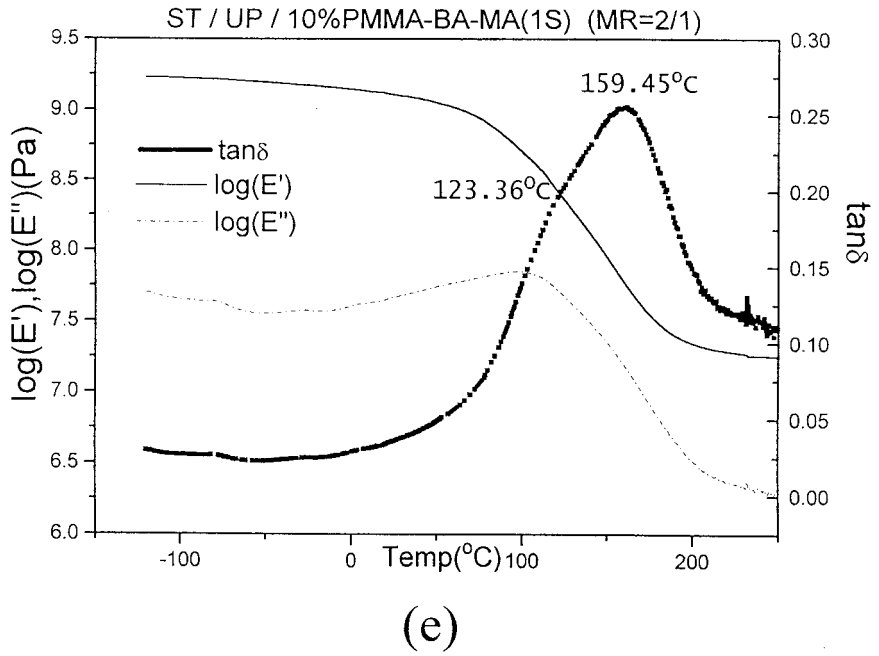

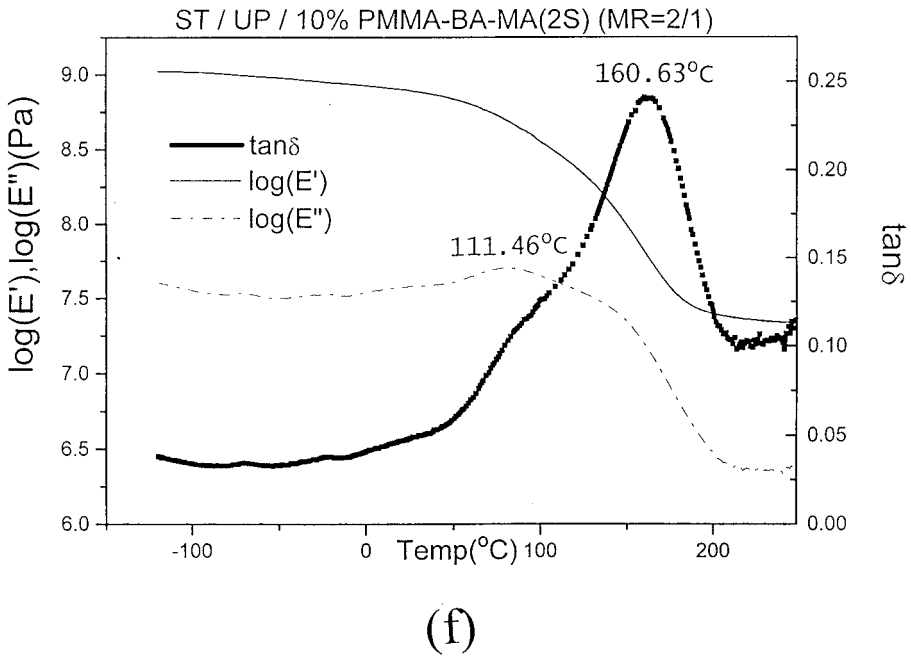

Figure 7 (*Continued from the previous page*)

BA–MA systems [Fig. 7(c–f)], T_{gR} (−17 to −24°C as measured by DSC) could be superposed with T_{g3}.

The addition of PMMA1S led to the most compatible ST/UP/LPA cured system, and the MR of ST consumed to polyester C═C bonds reacted (MR) deviated least from (less than) 2 : 1 in the major continuous phase P_1, which led to the highest crosslinking density in that phase because of the lowest shielding wall effect. The best crosslinking density effect of the P_1 phase itself resulted in the highest T_g (165.1°C) for the P_1 phase among the cured systems (Table V), which was even higher than that of the neat UP resin system at MR = 2 : 1 (162.4°C). This was ascribed to the fact that the LPA-induced globule microstructure

during the cure could enhance the final conversion of polyester C═C bonds,[15] leading to the enhancement of the crosslinking density and, in turn, an increase in T_g.

However, the addition of MMA–BA–MA caused a more compatible cured system compared to the addition of MMA–BA; yet, the T_g in the P_1 phase for the former system was lower. With a fixed LPA type, the addition of a higher MW LPA could cause a more incompatible ST/UP/LPA system [see Fig. 1(a–d)], but either a higher T_g (MMA–BA–MA system) or a lower T_g (PMMA and MMA–BA systems) in the P_1 phase was observed.

All of these were ascribed to the fact that for a less compatible ST/UP/LPA system, the plasticization effect of the R phase on the P_1 phase was less, and the crosslinking density in the P_1 phase itself was also lower. Because the lower plasticization effect was favorable for the increase of T_g in the P_1 phase, whereas the concomitant lower crosslinking effect was unfavorable, the T_g in the P_1 phase may have then depended on the relative importance of the two opposing effects. As the crosslinking effect was more significant, a more compatible ST/UP/LPA system led to a higher T_g in the P_1 phase, whereas the trend may have been reversed as the plasticization effect was more important. Apparently, either a highly compatible ternary system with a glassy LPA added, such as the PMMA system, or a highly incompatible ternary system (despite a rubbery LPA added), such as the MMA–BA system, pertained to the former case (i.e., the crosslinking effect predominant), whereas a somewhat incompatible ternary system with a rubbery LPA added (e.g., the MMA–BA–MA system) was categorized as the latter case (i.e., the predominant plasticization effect).

CONCLUSIONS

The phase-separation characteristics of ST/UP/LPA systems during the cure, as revealed by cured-sample morphology and the DSC reaction rate profile, could generally be predicted by the calculated molecular polarity difference between the UP resin and LPA. For the ST/UP/LPA system, the sample solution containing PMMA was the most compatible during the cure at 110°C, followed by that containing MMA–BA–MA and that containing MMA–BA. The most incompatible MMA–BA system exhibited a pronounced shoulder before the peak in the DSC rate profile because the onset of the gel effect in the major continuous phase occurred first and that of the LPA-dispersed phase lagged behind. With a fixed LPA type, the addition of a higher MW LPA caused a more incompatible ST/UP/LPA system, which led to a relatively lower peak reaction rate, a broader peak in the DSC rate profile, and a generally lower final conversion of total C═C bonds after the cure.

As a result of phase separation during the cure of the ST/UP/LPA system, the total α was a summation of the α in each phase, which depended on the shielding wall effect and the glass-transition effect therein. The former effect was controlled by the MR of ST to polyester C═C bonds in each phase (i.e., MR_{Pi}), whereas the latter effect was controlled by ΔT_{Pi}. Because the final conversion depended on the combination of the fractionation of different species among different phases and the vitrification of one or more of these phases, no prediction could be made with regard to the effect of LPA type on the final conversion for the systems studied.

For cured neat UP resin system without LPA, both $T_{g1\alpha}$ and $T_{g1\beta}$ for the polyester segments between the crosslinks reached a maximum at MR = 2 : 1. The higher the MR of ST to polyester C═C bonds (MR) was, the higher the degree of crosslinking was along the polyester chain, which led to higher $T_{g1\alpha}$ and $T_{g1\beta}$ values, and the longer the ST bridge between the crosslinks was, which led to lower $T_{g1\alpha}$ and $T_{g1\beta}$ values. A good balance of these two factors at MR = 2 : 1 resulted in an optimum crosslinking density, and, in turn, the highest $T_{g1\alpha}$ and $T_{g1\beta}$ values.

The T_g of the LPA and the phase-separation behavior during the cure may have influenced the T_g's for the ST/UP/LPA cured systems. On the basis of the proposed Takayanagi mechanical models, the T_g's in the major continuous phase of ST-crosslinked polyester (P_1 phase) for ST/UP/LPA systems were demonstrated to depend on the relative importance of the two opposing effects, namely, the plasticization effect of the R phase on the P_1 phase and the crosslinking effect of the P_1 phase itself in terms of the MR of ST consumed to polyester C═C bonds reacted. A more incompatible ST/UP/LPA system led to a lower plasticization effect and a concomitant lower crosslinking effect, the former of which was favorable for the increase of T_g in the P_1 phase and the latter of which was unfavorable.

References

1. Bartkus, E. J.; Kroekel, C. H. Appl Polym Symp 1970, 15, 113.
2. Atkins, K. E. In Sheet Molding Compounds: Science and Technology; Kia, H. G., Ed.; Hanser: New York, 1993; Chapter 4.
3. Suspene, L.; Fourquier, D.; Yang, Y. S. Polymer 1991, 32, 1593.
4. Hsu, C. P.; Kinkelaar, M.; Hu, P.; Lee, L. J. Polym Eng Sci 1991, 31, 1450.
5. Huang, Y. J.; Su, C. C. J Appl Polym Sci 1995, 55, 323.
6. Huang, Y. J.; Jiang, W. C. Polymer 1998, 39, 6631.
7. Huang, Y. J.; Chu, C. J.; Dong, J. P. J Appl Polym Sci 2000, 78, 543.
8. Lam, P. W. K. Polym Eng Sci 1989, 29, 690.
9. Bucknall, C. B.; Partridge, I. K.; Phillips, M. J. Polymer 1991, 32, 786.

10. Park, M. B. C.; McGarry, F. J. Proceedings of the 48th Annual Conference, Cincinnati, OH; SPI Composites Institute: New York, 1993; p 10B.
11. Huang, Y. J.; Chen, L. D. Polymer 1998, 39, 7049.
12. Huang, Y. J.; Lee, S. C.; Dong, J. P. J Appl Polym Sci 2000, 78, 558.
13. Podszun, W.; Suling, C.; Alberts, H. U.S. Pat. 4,369,296 (1983).
14. Chern, C. S.; Hsu, H. J Appl Polym Sci 1995, 55, 571.
15. Huang, Y. J.; Su, C. C. J Appl Polym Sci 1995, 55, 305.
16. Huang, Y. J.; Wen, Y. S. Polymer 1994, 35, 5259.
17. Krevelen, D. W. V. Properties of Polymers, 3rd ed.; Elsevier: London, 1990; pp 198, 323.
18. Fendor, R. F. Polym Eng Sci 1974, 14, 147.
19. Lecointe, J. P.; Pascault, J. P.; Suspene, L.; Yang, Y. S. Polymer 1992, 33, 3226.
20. Huang, Y. J.; Su, C. C. Polymer 1994, 35, 2397.
21. Takayanagi, M.; Imada, K.; Kajiyama, T. J Polym Sci Part C: Polym Symp 1966, 15, 263.
22. Ward, I. M.; Hadley, D. W. An Introduction to the Mechanical Properties of Solid Polymers; Wiley: New York, 1993; p 154.
23. Sperling, L. H. Introduction to Physical Polymer Science, 3rd ed.; Wiley: New York, 2001; p 438.
24. Huang, Y. J.; Lee, L. J. AIChE J 1985, 31, 1585.
25. Horie, K.; Mita, I.; Kambe, H. J Polym Sci Part A-1: Polym Chem 1969, 7, 2561.
26. Huang, Y. J.; Hsu, T. J.; Lee, L. J. Polymer 1985, 26, 1247.
27. Hsu, C. P.; Lee, L. J. Polymer 1993, 34, 4506.
28. Huang, Y. J.; Chen, C. J. J Appl Polym Sci 1993, 47, 1533.
29. Lee, S. C. M.S. Thesis, National Taiwan University of Science and Technology, 1998.
30. Cook, W. D.; Delatycki, O. J Polym Sci Polym Phys Ed 1974, 12, 2111.
31. Cook, W. D.; Delatycki, O. J Polym Sci Polym Phys Ed 1974, 12, 1925.
32. Lucas, J. C.; Borrajo, J.; Williams, R. J. J. Polymer 1993, 34, 3216.